Reactive and Functional Polymers 164 (2021) 104912

Contents lists available at ScienceDirect

Reactive and Functional Polymers

journal homepage: www.elsevier.com/locate/react

Perspective Article

Development of terpene based sorbents via emulsion templating: Synthesis and swelling behavior

Burcu Kekevi [a,*], E. Hilal Mert [b,*]

[a] Yalova University, Yalova Community College, Material and Material Processing Department, 77100 Yalova, Turkey
[b] Yalova University, Faculty of Engineering, Department of Polymer Materials Engineering, 77200 Yalova, Turkey

ARTICLE INFO

Keywords:
Terpene
β-Myrcene
High internal phase emulsion
Polymeric sorbent
Swelling behavior

ABSTRACT

Polymeric sorbent materials exhibiting excellent swelling capacity were developed using high internal phase emulsion (HIPE) templating approach. Precursor HIPEs were prepared by using continuous phases that composed of mixtures of β-myrcene (monomer) and 1,3-butanediol dimethacrylate (crosslinker). The influence of β-myrcene concentration on the emulsion stability and crosslinking was investigated. Swelling behaviors of resulting polyHIPEs in different solvents were studied. It was found that the maximum swelling capacities were reached 713%, 667% and 310% in benzene, toluene and hexane, respectively.

1. Introduction

Marine oil spills are one of the most threatening pollution to ecology and the environment. It is known that oil spills can cause serious damages on the health of marine creatures and humans [1,2]. Thereby, an effective and fast removal approach is necessary to eliminate and minimize the probable damages. For this purpose, several methods including chemical treatment with demulsifiers or dispersants [3,4], bioremediation with biological agents or microorganisms [5–7], and physical treatment with absorbents [8–10] have been used by the scientists. Among these, sorption is the most preferred one due to the ease of applicability and is driving scientists to develop effective new sorbent materials [11–13].

So far, scientists utilized several kinds of sorbent materials including inorganic kinds [14–16], biobased materials [17–19], synthetic polymers [12,13,20–22], and polymer composites that are combining inorganic species with polymer matrices [23]. However, all the above-mentioned sorbents have their own drawbacks. For instance, natural inorganic materials exhibit poor oil/water selectivity and low oil absorption capacities, while biobased organic sorbents usually have poor surface hydrophobicity, low removal efficiency, and buoyancy. On the other hand, in most of the cases synthetic polymer-based sorbents have poor biodegradability and biocompatibility [24]. Moreover, their relatively high density as compared to oils causes submerge of the sorbent material in the used environment during the utilization. Regarding to properties and efficiency, excellent oil-sorption capacity, ease of preparation, sustainability and low fabrication cost are the most demanded properties from a sorbent material [11].

In the last two decades, high internal phase emulsion templating (HIPE) approach has been attracting interest of scientist for the preparation of highly porous monolithic polymers. A HIPE is a concentrated emulsion consisting of minimum 74.05 vol% of internal phase. When monomeric species are used for the preparation of a HIPE, polymerization of the obtained emulsion leads the formation of polyHIPEs, which are highly porous and low-density materials [25]. So far, various types of polyHIPEs have been described by researchers for the sorption purposes including synthetic polymer based polyHIPEs [26–28] and bio-based polyHIPEs [29–32]. However, within our knowledge a terpene-based polyHIPE sorbent has not been reported yet.

Terpenes are a highly aromatic class of compounds that determine the scent of many herbs such as lavender, rosemary, citrus fruits. The simple derivation of these bio-based organic compounds from the essential oils of citrus and hemp plants has made terpenes one of the most widely preferred sustainable materials in fragrances, cosmetics, food, pharmaceuticals and inhalation products [33,34]. Due to the wide availability in nature and inherent double bonds in the chemical structure of mono-, di-, tri- and other polyterpenes, the demand on the studies on creating novel sustainably sourced polymeric products by using terpenes and terpenoids have been also increased lately [35]. In this respect, we also focused on the development of terpene-based sorbent polymers via emulsion templating approach. The depletion of fossil resources has increased the importance given to the concept of

* Corresponding authors.
E-mail addresses: bkekevi@yalova.edu.tr (B. Kekevi), hmert@yalova.edu.tr (E.H. Mert).

https://doi.org/10.1016/j.reactfunctpolym.2021.104912
Received 12 February 2021; Received in revised form 5 April 2021; Accepted 14 April 2021
Available online 17 April 2021
1381-5148/

sustainability and the focus of scientists has shifted to renewable monomers, solvents and additives. Terpenes, which are widely found in nature as different species, are stated as interesting renewable monomers . Isoprene-like chemical structure of terpenes made these organic molecules to be preferred especially in applications requiring elasticity. Three double bonds present in the chemical structure of β-myrcene provides relatively high reactivity to the structure, so that it can be even polymerized at room temperature without using a polymerization catalyst [36]. The functionality of the pendant double bonds in its structure makes β-myrcene an alternative chemical that can be used in a variety of applications. For instance, it has found use as a hardening agent for polyurethane [37], raw material for disposable absorbent materials [38], or pure polymers for biomedical applications [39] in studies conducted so far. Despite so many studies focusing on the polymerization of β-myrcene have been performed, free radical copolymerization of this terpene in HIPE templates has not yet been studied in detail.

β-Myrcene and ethylene glycol dimethacrylate (EGDMA) based polyHIPEs [40] and polyHIPE/nanoclay nanocomposites [41] were first synthesized by our group in the literature. By these studies, it was shown that when the ratio of β-myrcene in the monomer mixture exceeded a critical limit resulting polyHIPEs demonstrated an elastic behavior. In addition, it has been observed that during the polymerization of these precursor HIPEs, volume contraction occurs, resulting in cavities collapsing and capillary channels remained behind.

Based on these premises, this work focused on the purpose of preparing elastic polymer monoliths with excellent swelling behavior. For this purpose, copolymerization of β-myrcene with 1,3-butanediol dimethacrylate (BDDMA) was achieved in HIPE templates. Consequently, polyHIPE sorbents with excellent swelling capacity were prepared by implementing a bio-derived monomer. Resulting polyHIPEs were prepared as the specifically designed materials for spilled oil recovery applications. To the best of our knowledge, these are the first examples of β-myrcene based polyHIPE sorbents in the literature.

2. Experimental

2.1. Materials

β-Myrcene (technical grade, Sigma-Aldrich), 1,3- butanediol dimethacrylate (BDDMA; 95%, contains 200–300 ppm MEHQ as inhibitor, Sigma-Aldrich), poly(ethylene glycol)-*block*-poly(propylene glycol)-*block*-poly(ethylene glycol) (Pluronic® L-121; Mn ~ 4400, non-ionic surfactant, Sigma-Aldrich), sorbitane monooleate (Span® 80, non-ionic surfactant, Sigma-Aldrich), potassium persulfate (KPS; ≥99.0%, ACS reagent), calcium chloride hexahydrate ($CaCl_2.6H_2O$; 98%, Sigma-Aldrich), benzene (anhydrous, 99.8%, Sigma-Aldrich), toluene (≥99.5%, ACS reagent), n-hexane (anhydrous, 99.5%, Sigma-Aldrich), tetrahydrofuran (THF; anhydrous, ≥99.9%, inhibitor-free, Sigma-Aldrich) were used as received. In all experiments ultrapure double distilled deionized water was used.

2.2. Synthesis of terpene-based polyHIPE sorbents

Terpene-based polyHIPE sorbents were all prepared with 80 vol% of nominal porosity. Accordingly, 40 mL of each HIPE was the aqueous phase, while 10 mL was the continuous (external/oil) phase. HIPEs were prepared by using a reactor system composed of a round bottom two-necked glass flask equipped with an overhead stirrer and a peristaltic pump. In a typical experiment, continuous phase was consisting β-myrcene, BDDMA, Pluronic® L121 and Span® 80; while the internal phase was obtained by dissolving 1 wt% of $CaCl_2.6H_2O$ and 1 mol% of KPS (regarding to monomers) in deionized water. HIPEs were prepared under continuous stirring (@400 rpm). For this purpose, 40 mL of internal phase was dispersed in the continuous phase by using a peristaltic pump at a pumping rate of 50 rpm. Once the addition of internal phase completed, stirring was continued for an additional 15 min in order to obtain a homogenous dispersion of emulsion droplets. Afterwards, obtained HIPE was poured into a glass flask and polymerized in an air-circulated oven at 60 °C for 24 h. Thereafter, resulting cylindrical monolith was removed from the glass flask and Soxhlet extracted by using ethanol for 24 h, and dried in a vacuum oven at 40 °C until constant weighing was available. In order to demonstrate the influence of drying on the pore morphology, a series of polyHIPEs sorbents were also prepared according to the given procedure above and freeze-dried.

During the experiments the ratio of β-myrcene to BDDMA was changed between 85:15 and 99:1. In addition, total amount of the surfactants was corresponding to the 30 vol% of the continuous phase. The ratios of the Span® 80 and Pluronic® L121 were determined based on the volume ratios of the myrcene and BDDMA monomers in the continuous phase, respectively. In the end, three different polyHIPE sorbents were obtained by using five different precursor HIPE templates. Resulting materials were named as PMBS-x, in where x is the formulation number of the used HIPE template. Compositions of the emulsion phases of the precursor HIPE templates are presented in Table 1.

2.3. Solubility test

The amount of soluble polymer parts in the resulting polyHIPEs was determined by applying solubility test. In this respect, certain amounts of polyHIPE sorbents weighed in a glass reactor, and 20 mL of THF was added on. The mixture was stirred at room temperature for 24 h.

Table 1
Compositions of the emulsion phases of the precursor HIPE templates.

Emulsion Phase	Composition		Ratio (vol%)	mmol
HIPE-1				
External (Oil)	β-Myrcene		85	49.35
	BDDMA		15	6.70
	Emulsifier	*Span® 80*	25.5	5.89
		Pluronic® L121	4.5	10.29×10^{-2}
Internal	Deionized Water (mL)		40	
	$CaCl_2.6H_2O$ (g)		0.40	
	KPS		5.99×10^{-2}mmol	
HIPE-2				
External (Oil)	β-Myrcene		90	52.25
	BDDMA		10	4.46
	Emulsifier	*Span® 80*	27	6.24
		Pluronic® L121	3	6.85×10^{-2}
Internal	Deionized Water (mL)		40	
	$CaCl_2.6H_2O$ (g)		0.40	
	KPS		5.36×10^{-2}mmol	
HIPE-3				
External (Oil)	β-Myrcene		95	55.16
	BDDMA		5	2.23
	Emulsifier	*Span® 80*	28.5	6.58
		Pluronic® L121	1.5	3.43×10^{-2}
Internal	Deionized Water (mL)		40	
	$CaCl_2.6H_2O$ (g)		0.40	
	KPS		6.61×10^{-2}mmol	
HIPE-4				
External (Oil)	β-Myrcene		97	56.32
	BDDMA		3	1.33
	Emulsifier	*Span® 80*	29.1	6.72
		Pluronic® L121	0.9	2.05×10^{-2}
Internal	Deionized Water (mL)		40	
	$CaCl_2.6H_2O$ (g)		0.40	
	KPS		6.74×10^{-2}mmol	
HIPE-5				
External (Oil)	β-Myrcene		99	57.48
	BDDMA		1	0.44
	Emulsifier	*Span® 80*	29.7	6.86
		Pluronic® L121	0.3	6.86×10^{-2}
Internal	Deionized Water (mL)		40	
	$CaCl_2.6H_2O$ (g)		0.40	
	KPS		6.93×10^{-2}mmol	

Afterwards, samples were filtered, extracted with ethanol for 10 h and dried under vacuum until constant weighing was available.

2.4. Characterization

Porous morphology of the polyHIPEs was characterized by scanning electron microscopy (SEM; ZEISS Supra 40 VP, Germany). With this aim, polyHIPE samples were coated with gold prior to analysis. The Brunauer-Emmet-Teller (BET) specific surface area (δ_{BET}) of the polyHIPEs was measured by using Micromeritics Gemini VII Surface Area and Porosity Analyzer (Micromeritics Instrument Corporation, USA). Measurements were performed after degassing procedure, which was conducted at 100 °C for 24 h, under nitrogen flow on a degassing unit (Micromeritics FlowPrep 060 Sample Degas Unit, Micromeritics Instrument Corporation, USA). For each sample, δ_{BET} was calculated as the arithmetic average of 3 different measurements that were conducted by using 3 different specimens.

Foam densities (ρ_f) of the obtained polyHIPEs were determined according to Archimed's principle. For this purpose, an analytical balance equipped with a density determination kit (Sartorius YDK01) was used. For each sample, foam density was calculated as the arithmetic average of 3 different measurements which were conducted by using 3 different specimens.

Elastic modulus of the polyHIPEs was determined in terms of compressive properties. For this purpose, stress vs. strain curves of the monolith samples with the dimensions of ~1.5 cm × 1.0 cm were recorded on a ZwickRoell Z020 Universal Testing Machine (ZwickGmbH&Co.KG, Germany) equipped with a 10 kN load cell. Elastic modulus of the samples was calculated from the stress vs. strain curves by using testXpert II Testing Software (ZwickGmbH&Co.KG, Germany). For each sample five different specimens were used in compression tests, and polyHIPEs were tested without applying any cutting or breaking operations.

2.5. Swelling behavior

Maximum swelling capacities of the polyHIPE sorbents were determined in different solvents. For this aim, benzene, toluene and n-hexane were chosen as solvent media. In a typical swelling test polyHIPE sorbent sample was thrown into 20 mL of solvent at 25 °C, and the weight of the sorbent was measured in constant time intervals, after the sample was dried with a napkin. Once the constant weighing was reached swelling capacities were calculated by using the following equation.

$$Swelling\% = (w_{max} - w_0) \times 100/w_0 \quad (1)$$

where w_{max} refers to the maximum weight of the polyHIPE sample during swelling, whereas w_0 stands for the initial weights of polyHIPE samples.

2.6. Reusability

In order to determine reusability of the polyHIPEs, certain weights of polyHIPE sorbents was immersed in solvents and benzene/water mixture and left in 24 h to reach maximum absorbance capacity. Then polyHIPEs were removed by filtering and dried in a vacuum oven at 40 °C for 24 h to release the absorbed solvent. The absorption/desorption cycles were repeated 10 times.

3. Results and discussion

In order to implement high amount of a bio-derived monomer and to obtain polyHIPEs exhibiting elasticity and high swelling capacity, the ratio of β-myrcene in the continuous phase of precursor HIPE templates were derived between 85 vol% and 99 vol%. Considering the different polarities of β-myrcene and BDDMA a bisurfactant system was used to ensure the stability of precursor HIPE templates. In this respect, mixtures of Span® 80 and Pluronic® L121 were used in each formulation. The ratio of the surfactants was determined based on the ratio of the monomers in the oil phase by keeping the total surfactant concentration constant. The stability of the obtained emulsions was evaluated at room temperature and polymerization conditions. Accordingly, observations regarding to emulsion stability are summarized in Table 2. It was determined that using a surfactant mixture was very effective for forming stable HIPEs of β-myrcene and BDDMA. Both at lower and higher concentrations of β-myrcene same result was obtained in terms of stability. On the other hand, HIPEs containing higher β-myrcene concentrations exhibited significantly high viscosity. When the β-myrcene ratio exceeded 95 vol%, even continuing the stirring process became quite difficult. For all precursor HIPEs stability of the emulsions was maintained for more than 72 h at room temperature. Moreover, we did not observe phase separation during polymerization period for any of the HIPEs. However, in the end, HIPEs containing 97 vol% and 99 vol% of β-myrcene were not crosslinked. Accordingly, solid monolithic structures produced from HIPE-4 and HIPE-5 is non-existent; HIPE-4 and HIPE-5 resulted in gel-like creams (Table 2). In addition, significant volume shrinkage was observed during drying of the solvent extracted monoliths that were produced from HIPE-1, HIPE-2, and HIPE-3. This result could be explained by the reactivity of β-myrcene in the copolymerization medium. On the other hand, in free radical polymerization, crosslinking is only formed through a polymer radical whose concentration is fairly low and whose lifetime is very short. The existence of other chains of different ages during its growth has a significant effect on the kinetics of network formation [42]. On the other hand, since there is a crosslinking density, distribution of crosslinking degree is different at different domains of the polymer network [43]. In the copolymerization of monomers having different degrees of water solubility it is possible to observe inhomogeneous gels which contain different domains with different degrees of crosslinking. This situation usually occurs due to the combination of several parameters including the reactivity of the double bonds in the monomers and the decreased reactivity of the double bonds on the resulting polymer chains [42]. When a monomer unit is bound in the polymer chain its reactivity may change due to chemical and/or physical effects including steric hindrance and excluded volume effect. It is also important to know which primary polymer molecule the crosslinked divinyl monomer originally belonged to [43]. Accordingly, it is possible that the resulting polymer network exhibited macroscopic and microscopic inhomogeneities.

When copolymerization crosslinking of β-myrcene and BDDMA in precursor HIPEs was initiated with water-soluble KPS, radicals are generated in the aqueous internal phase upon the decomposition of the initiator. Since only a small amount of β-myrcene was dissolved in the internal phase, oligoradicals might have formed by the attack of initiator radicals to β-myrcene in this phase and precipitated when they reach the solubility limit. On the other hand, oligoradicals might penetrate to the water/oil interface, which is the locus of initiation, and to the oil

Table 2
Emulsion stability and crosslinking situation of the precursor HIPEs.

	β-myrcene: BDDMA	Stability@25 °C	Stability@60 °C	Crosslinking*
HIPE-1	85:15	>72 h	>24 h	+
HIPE-2	90:10	>72 h	>24 h	+
HIPE-3	95:5	>72 h	>24 h	+
HIPE-4	97:3	>72 h	>24 h	−
HIPE-5	99:1	>72 h	>24 h	−

* (+): crosslinked; (−): not crosslinked.

macrophase. Since the oil phase is rich in β-myrcene and BDDMA, it is expected that the polymerization is proceed in this phase. During polymerization the rate of addition of β-myrcene units to the primary radicals or the growing oligoradicals is different from the addition of BDDMA units. Since β-myrcene is highly reactive it tends to add its own monomer during copolymerization reactions [44]. In addition to all, despite β-myrcene has three double bonds, the resonance between the conjugated bonds might also prevent formation of crosslinking between β-myrcene and BDDMA [45]. On the other hand, previous findings of Abraham and Kollarigowda [36] might also explain the polymer network structure. Abraham and Kollarigowda reported that polymyrcene chains could easily form micro-crosslinks due to the unsaturated bonds. Based on their findings, the degree of micro-crosslinking is dependent on the concentration of β-myrcene and increases with the increasing amount of it [36]. Accordingly, the final polymer microstructure is a result of monomer reactivity and total monomer amount in the reaction system. At higher BDDMA concentrations macrocrosslinked polymer network can be formed, while at lower BDDMA concentrations the resulting polymer is composed of different domains with low degree of macro and micro-crosslinks. Thereby, most of the polymer network could be dissolve in solvents. However, low degrees of macro and micro-crosslinks could avoid fully collapse of the polyHIPE structure. On the other hand, the reason why HIPE-4 and HIPE-5 was not resulted in any solid polymer could be attributed to be the inhibition of micro-crosslinking. Since the reaction medium was highly viscous in these HIPEs, it is possible that either micro-crosslinking of the polymyrcene chains was not occurred due to the decreased diffusion of growing chains.

Pore morphology of the obtained polyHIPE sorbents was investigated by using SEM imagining. SEM micrographs are presented in Fig. 1. However, the SEM images presented in Fig. 1 are not coherent with the well-known hierarchical macroporous structure of polyHIPEs. The morphology is more consistent with polyHIPEs where cavities collapse during drying, which can be attributed to the low-crosslinking density [46–48]. It can be seen by comparing the SEMs at low and high magnifications given in Fig. 1A and B that collapsing of cavities accompanied with the volume contraction of the monoliths lead to capillary-like pores. The average sizes of these pores were calculated by measuring the diameter of a minimum of 60 pores from the SEM image (Mag = 5.00 K X) for each sample. The average pore sizes for PMBS-1, PMBS-2 and PMBS-3 were found to be 0.52 ± 0.03 μm, 1.10 ± 0.04 μm and 0.65 ± 0.04 μm, respectively.

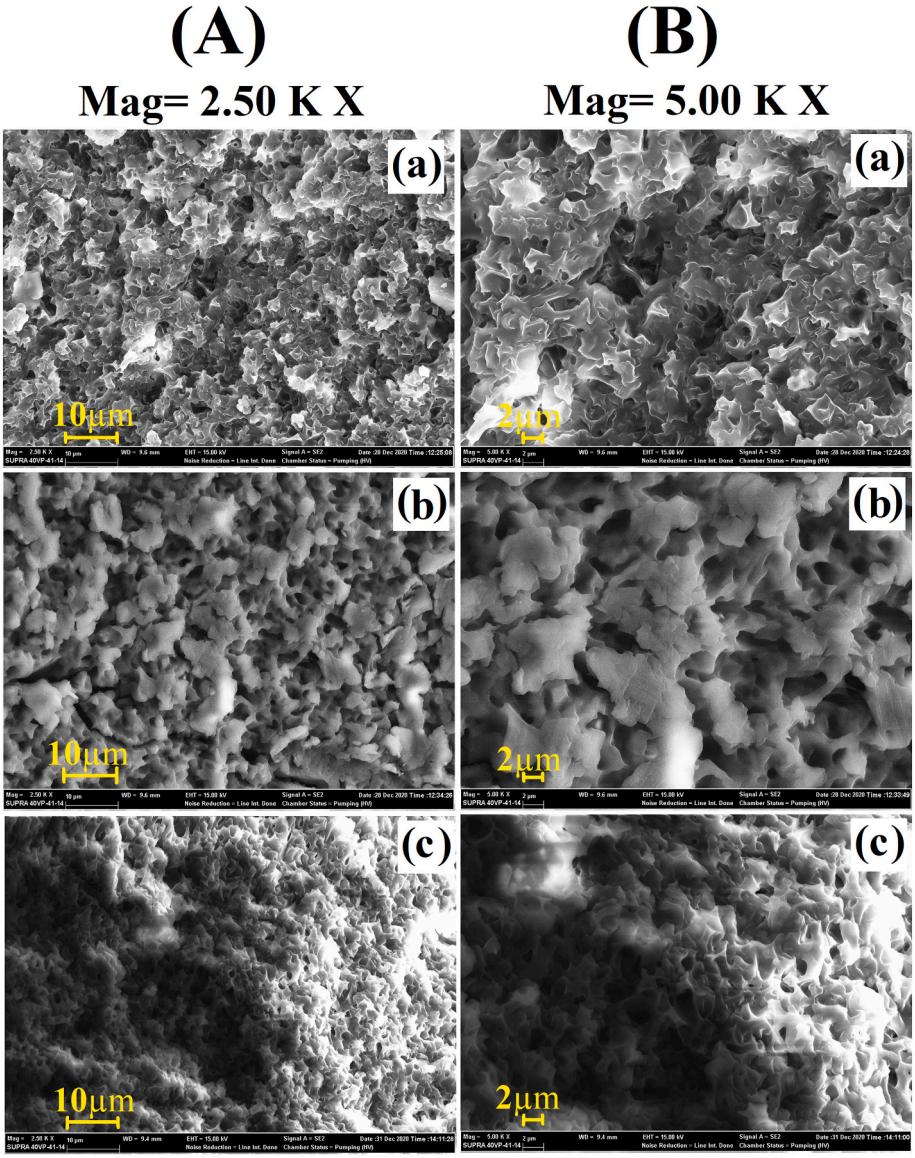

Fig. 1. SEM images of the Soxhlet extracted polyHIPEs: (A) Images at low magnificaiton, (B) Images at high magnification. (a) PMBS-1, (b) PMBS-2, (c) PMBS-3.

Collapse of well-known polyHIPE pore morphology can be attributed to the presence of high amount of β-myrcene in the continuous phase of precursor HIPEs and is consistent with our previous findings [40]. As the amount of β-myrcene was increased, the degree of macro-crosslinking might be decrease as explained above. Because of the low degree of crosslinking, volume of the resulting monoliths was contracted after solvent extraction and drying. Consequently, cavities were all collapsed, and capillary-like pores arise due to the volume shrinkage. On the other hand, as mentioned above micro-crosslinks might be the reason why the polyHIPE structure is not fully collapsed.

In order to confirm that the resulting morphology was arise due to the Soxhlet extraction followed by drying of the low-crosslinked polymer network, a series of polyHIPEs that were synthesized by using precursor HIPE-1, HIPE-2, and HIPE-3 formulations were freeze-dried. SEM images of the freeze-dried samples are also presented in Fig. 2A. It can be clearly seen from the SEM images of the freeze-dried samples that the crosslinker amount has a significant influence on the formation of open-porous morphology. As the ratio of β-myrcene in the HIPE formulation increased and the ratio of the crosslinker comonomer decreased the morphology was altered from open-cell to closed-cell. The polyHIPE sample in which β-myrcene/BDDMA ratio is 85/15 was found to be composed of cavities connected with pore throats. Although this example exhibits a limited openness, the sample with a monomer ratio of 90/10 was found to have a completely closed-cell structure. Moreover, the cavities in the sample synthesized from HIPE-3 were found to be collapsed completely. At this point, we should mention that apart from the other two samples, this sample was in a sticky form at the end of freeze-drying. In order to reveal the amount of soluble polymer parts, freeze-dried samples were treated with a solvent (THF) for 24 h at 25 °C and the weight loss of the samples were calculated. Accordingly, it was determined that the percentage of weight loss for the freeze-dried samples of PMBS-1, PMBS-2, and PMBS-3 after solubility test were 75.85%, 81.85%, and 73.21%, respectively. To demonstrate the influence of solubility test on the final pore structure of low-crosslinked polymer network, morphology of these samples was also investigated by SEM and presented in Fig. 2B. The images presented in Fig. 2B shown that treating freeze-dried polyHIPEs with an organic solvent leads much more open-porous structure. This result was demonstrated that, in addition to removing soluble polymer from the resulting polymer network, treating polyHIPEs with a solvent also benefits the removal of the internal phase entrapped in voids during the formation of continuous polymer film. On the other hand, this result is consistent with the hypothesis suggested by Menner and Bismarck about the formation of pore throats in HIPE templating [49]. It is known that pore structure of

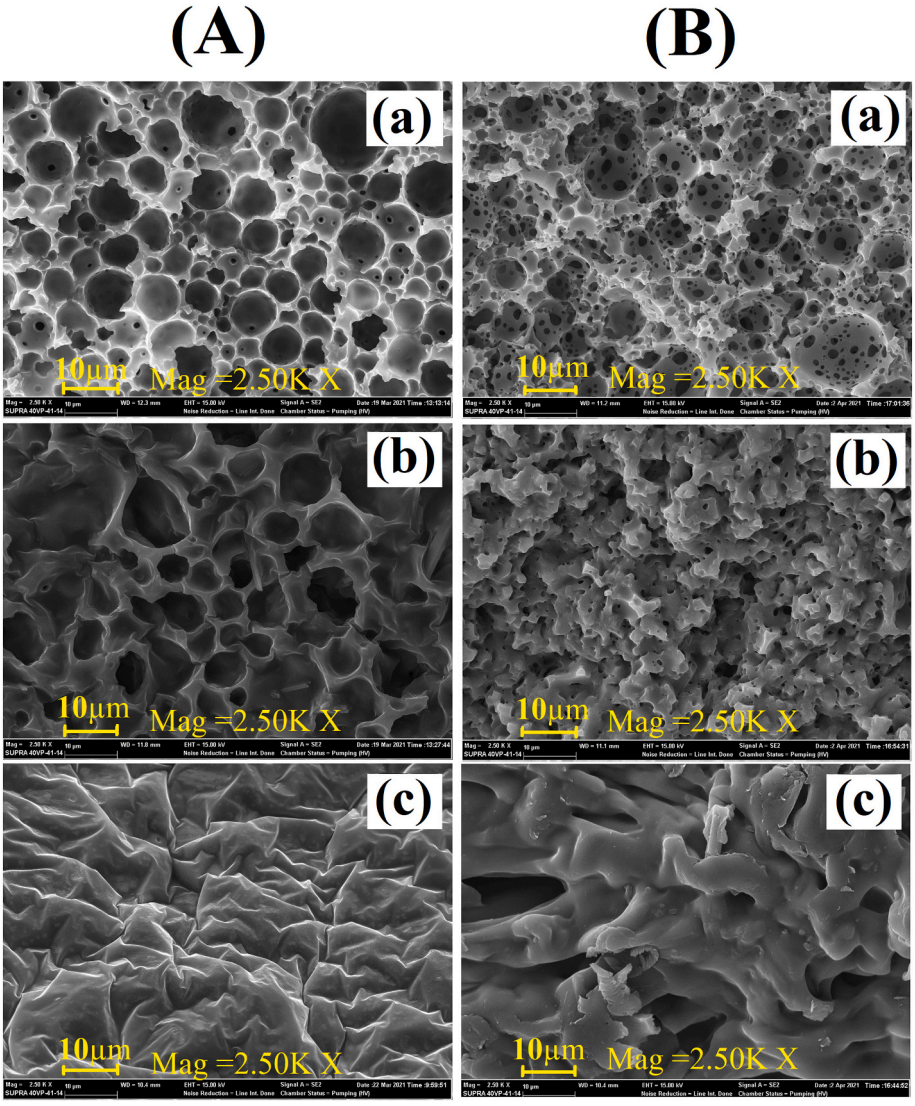

Fig. 2. (A) SEM images of the freeze-dried polyHIPEs and (B) SEM images taken after solubility test of the freeze-dried polyHIPEs. (a) PMBS-1, (b) PMBS-2, (c) PMBS-3.

polyHIPEs is dependent on several parameters including surfactant concentration, internal phase volume, emulsion stability, droplet size, monomer composition, and polymer film formation. According to Menner and Bismarck [49], aqueous phase droplets are entrapped within the organic polymer films that formed between the adjacent droplets during polymerization. The pore openings between the cavities are formed during the purification step (Soxhlet extraction and vacuum drying), as a result of the rupture of the thin polymer films around the adjacent droplets while the aqueous phase is removed from the obtained polyHIPE.

It appears that solvent treatment or Soxhlet extraction is still required to obtain a more open structure in polyHIPEs with sufficient crosslinking, even if the samples are freeze dried. On the other hand, it can be said that the purification technique will not cause a significant change in the pore structure of low-crosslinked polyHIPEs.

At this point, it was required to confirm the chemical structure of the resulting polyHIPEs. To confirm the crosslinking reaction between β-myrcene and BDDMA, chemical structures of the monomer, comonomer and resulting polyHIPEs were studied via FTIR and overlapped spectrums are presented in Fig. 3. In Fig. 3, the peak at 3092 cm^{-1} arise from = C—H stretching of β-myrcene and it disappeared by polymerization. Consecutive absorption peaks appeared at 2970 cm^{-1}, 2931 cm^{-1} and 2860 cm^{-1} in the spectrum of β-myrcene correspond to asymmetric stretching vibrations of —CH_3, —CH_2 and —CH. These peaks are observed as a broad band in the spectrum of polyHIPEs. Conjugated diene structure of β-myrcene located in C_1═C_2 and C_3═C_4 positions is verified by the peak appeared at 1594 cm^{-1} in the spectrum of β-myrcene. However, this peak is not so intense because of steric hindrance caused by the conjugated double bonds. On the other hand, not appearance of the absorption peak at 1594 cm^{-1} in the spectrums of polyHIPEs can be attributed to the crosslinking reaction. Additionally, the absorption frequencies at 890 cm^{-1} and 988 cm^{-1} are because of the sp^2 C—H bending of the double bonds of β-myrcene; while the former corresponds to di-substituted diene structure, the latter corresponds to mono-substituted alkene [50]. It was detected that the peak corresponding to the di-substituted diene structure was also appeared in the FTIR spectrums of polyHIPEs with a remarkably decreased intensity. On the other hand, the peak corresponding to the mono-substituted alkene structure was not observed in the FTIR spectra of the polyHIPEs. In addition to all, the peaks appeared at 1637 cm^{-1} and 1718 cm^{-1} in the spectrum of BDDMA corresponds to the —C═C— stretching vibrations and —C═O stretching of the monomer, respectively. It was also detected from the spectrums of polyHIPEs that the peak corresponding to —C═O stretching was appeared with a declined absorption frequency, while the peak corresponding to —C═C— stretching was found to be disappeared. Consequently, FTIR results are demonstrating that the crosslinking of β-myrcene with BDDMA was predominantly occurred via the mono-substituted alkene structure.

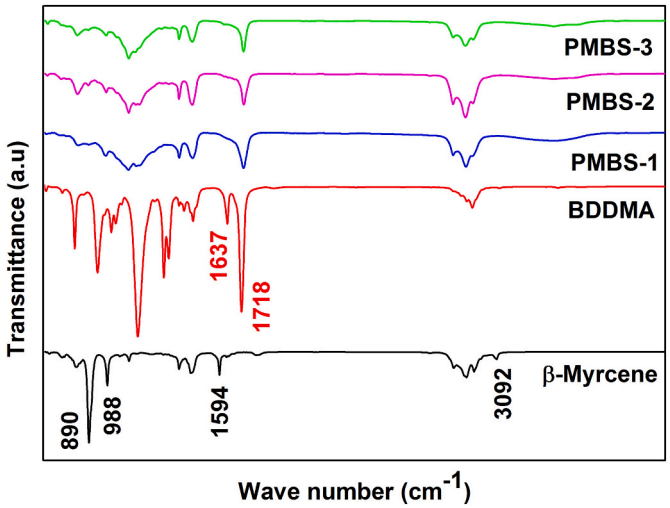

Fig. 3. FTIR spectrums of β-myrcene, BDDMA, and PMBSx sorbents.

The major advantage of using a comonomer having a spacer group is the decrease of steric hindrance of conjugated double bonds and the increase of polymerization ability of β-myrcene in the emulsion medium [51]. There is also an additional advantage of copolymerizing β-myrcene with BDDMA comonomer is that each monomeric unit contributes to the chain flexibility. In here, although high ratio of volume contraction was occurred in the resulting polyHIPEs, it was also observed that each sorbent exhibits rubbery behavior and reversible elastic deformation. As mentioned above, this result might mostly be attributed to the high reactivity of β-myrcene against BDDMA. As a consequent, polymerization of HIPE precursors resulted in polyHIPE sorbents with low ratio of crosslinks were obtained, as with rubbers.

The influence of the monomer composition was also investigated in terms mechanical properties. Mechanical properties of the obtained polyHIPEs were investigated via compression tests. Elastic modulus (Ec) of the samples that were determined from stress-strain plots were presented in Table 3, while the stress-strain plots were given in *Supplementary Information File* (Fig. S3). In addition, the elastic behavior of the obtained polyHIPEs can be clearly seen from the *Supplementary Video File*. It was determined by the compression tests that the elastic modulus of polyHIPEs was significantly decreased with the decreasing percentage of comonomer (BDDMA). As the ratio of BDDMA descended, elastic modulus of the polyHIPEs decreased, most probably due to the low crosslinking density. According to Table 3, elastic modulus of PMBS-1, PMBS-2, and PMBS-3 was found to be 431.50 kPa, 377.01 kPa, and 271.50 kPa, respectively. Although resulting polyHIPEs did not exhibit high mechanical performance, these results are consistent with the previously reported polymyrcene based polymers [55–57].

In Table 3, Specific BET surface area (δ_{BET}) and foam density (ρ_f) of the resulting polyHIPEs tabulated. It was determined that obtained polyHIPEs were exhibited similar foam densities which were below 1.0 g cm^{-3}. However, δ_{BET} values of the polyHIPEs were even found to be lower than conventional polyHIPEs, which is not a surprising result considering the final morphology of the materials [52–54]. According to Table 3, specific surface area of the polyHIPEs was found to be decrease as the ratio of β-myrcene increased. This result is consistent with the pore morphologies of the resulting polyHIPEs.

Considering the highly flexible structure of the obtained monoliths, swelling behaviors in different solvents were investigated. The swelling of a gel can be defined as the compatibility of solvent molecules with the polymer structure in solution. And generally, swelling occurs if the solvent used has a similar polarity value to the polarity of the polymer surface [58–60]. β-Myrcene is a highly hydrophobic molecule and polyHIPE sorbents synthesized with high amounts of β-myrcene are showing highly hydrophobic behavior. Due to their high hydrophobicity of the polyHIPEs, benzene, toluene, and n-hexane were preferred as the solvent media of swelling experiments. In addition, absorption capacities were also investigated in benzene/water mixtures (4 mL benzene in 10 mL deionized water) to reveal the absorption performance of the sorbents in aqueous environment. The absorption capacities of polyHIPEs in different solvents and benzene/water mixture are given in Table 4. In addition, photographs of the polyHIPEs taken before and after absorption (in toluene) are presented in the *Supplementary*

Table 3
Specific BET surface area (δ_{BET}), foam density (ρ_f), and elastic modulus (Ec) of the polyHIPE sorbents.

	δ_{BET} (m^2g^{-1})	ρ_f (gcm^{-3})	Ec (kPa)
PMBS-1	0.33	0.95	431.50 ± 25.81
PMBS-2	0.10	0.94	377.01 ± 16.45
PMBS-3	0.04	0.95	271.50 ± 12.37

Table 4
Maximum swelling capacities of the polyHIPEs.

	Toluen (%)	Hexane (%)	Benzene (%)	Benzene/Water (%)
PMBS-1	713.86 ± 19.25	309.76 ± 18.79	667.18 ± 29.76	623.45 ± 18.61
PMBS-2	573.12 ± 41.58	245.3 ± 16.38	570.67 ± 10.97	484.53 ± 10.25
PMBS-3	418.50 ± 20.87	179.5 ± 12.38	434.19 ± 16.12	413.32 ± 12.27

Information File (Fig. S1 and Fig. S2).

When the maximum swelling capacities of the polyHIPEs in toluene, hexane, benzene, and benzene/water mixtures was compared, the order of swelling was found to be PMBS-1 > PMBS-2 > PMBS-3. Meanwhile, the amount of BDDMA in the monomer mixture of precursor HIPEs was 15 vol%, 10 vol%, and 5 vol% for PMBS-1, PMBS-2, and PMBS-3, respectively. According to this result, polyHIPE which was obtained by using the HIPE containing higher amount of BDDMA has the maximum swelling capacity. This result is consistant with the literature: It is known from the previous studies that acrylate monomers having long-chain alkyl groups exhibit good affinity towards organic solvents [61]. On the other hand, since the relative polarities of the solvents are changing on the order of benzene > toluene > hexane, it was expected that the solvent with highest polarity shows maximum absorption. Interestingly, the maximum amount of absorption for the solvents was found to be changed in the order of toluene > benzene > hexane for PMBS-1, and toluene ≈ benzene > hexane for PMBS-2. On the other hand, maximum amount of absorption was changing in the order of benzene > toluene > hexane for PMBS-3. According to the swelling capacities of polyHIPEs in benzene/water mixtures (Table 4), each polyHIPE showed significant swelling also in the presence of water. The maximum swelling capacities of polyHIPEs in benzene/water mixtures was found to be 623.45%, 484.53% and 413.32% respectively for PMBS-1, PMBS-2, and PMBS-3. These results suggest that the polyHIPEs can be used in aqueous environment.

Based on the Flory's swelling theory, the elasticity, affinity to solvent and crosslinking density is the primary parameters that control the swelling capacity of the sorbent materials [62]. In polyHIPE sorbents composed of polymer chains with higher amounts of β-myrcene units than BDDMA units, the elasticity of the material increased while the crosslinking density is decreased. This situation has led to the formation of polymer networks which are more prone to expansion. Contrary to this, swelling capacity of the obtained polyHIPE sorbents was found to be decrease with the decrease of the amount of crosslinker comonomer, BDDMA. The reason of this diminishment in swelling capacity might be attributed to the tight arrangement of β-myrcene units and the formation of micro-crosslinked structure in the polymer network to constitute an elastomeric structure [36].

In order to demonstrate the reusability of the resulting materials, polyHIPEs were tested in absorption/desorption experiments through 10 cycles. The variation of maximum absorption capacities of each polyHIPE sorbent during 10 cycles were demonstrated in Fig. 4. It can be seen from Fig. 4 that each polyHIPE can be effectively used to remove benzene through 6 cycles, toluene through 5 cycles, and hexane and benzene/water mixture through 3 cycles. SEM imagening was used to determine the pore structure of the polyHIPEs after 10 cycles of absorption/desorption tests. For this purpose, pore morphologies of the

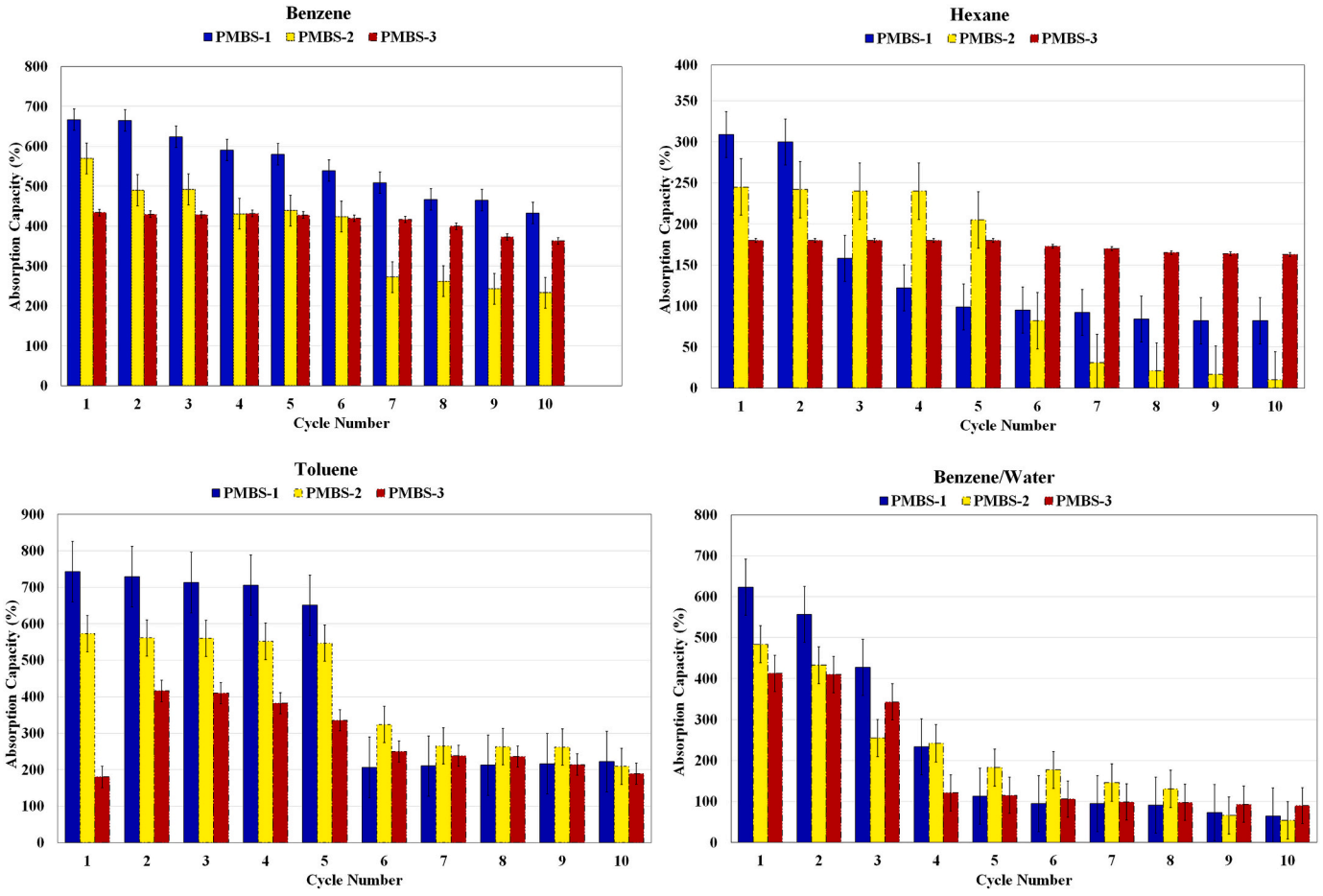

Fig. 4. Aborption capacities of polyHIPEs at different absorption/desorption cycles.

polyHIPEs that were used in toluene absorption were investigated and SEM images are presented in Fig. 5. It can be seen from the images given in Fig. 5 (a) and (b) that PMBS-1 and PMBS-2 exhibited small pores and pore structure of these samples did not deformed during adsorption/desorption cycles. On the other hand, Fig. 5 (c) reveals that the morphology of PMBS-3, which has the lowest crosslinking degree, was found to be significantly deformed.

Kinetic analysis of solvent absorption with polyHIPEs was also investigated and absorption kinetics of the sorbents was presented in Fig. 6. The given kinetic curves were obtained by plotting the absorption capacity against the contact time of the polyHIPEs with the studied solvents. When Fig. 6 is evaluated, it can be said that PMBS-1 sorbent reaches saturation in 2 h, while PMBS-2 and PMBS-3 sorbents reach saturation in 3 h and 7 h, respectively. It is also clear that the curves of polyHIPEs remained constant until the end of the experiments after reaching the saturation point.

In order to make a complete assessment of the absorption kinetics, the kinetic data obtained experimentally was fitted into pseudo first-order and pseudo-second order kinetic model by using the linearized

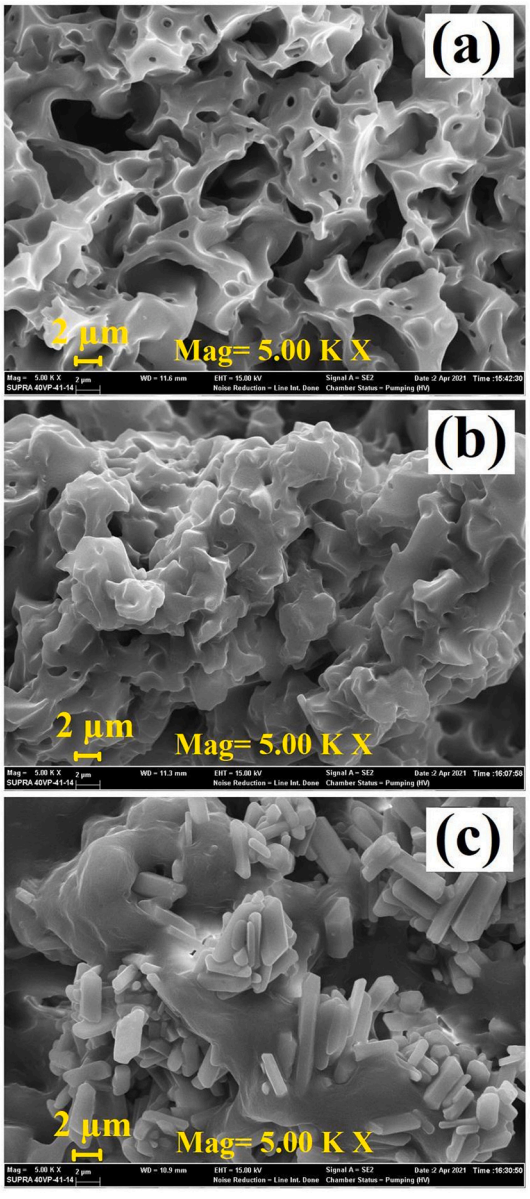

Fig. 5. SEM images of polyHIPEs after performing 10 cycles of absorption/desorption in toluene: (a) PMBS-1, (b) PMBS-2, and (c) PMBS-3.

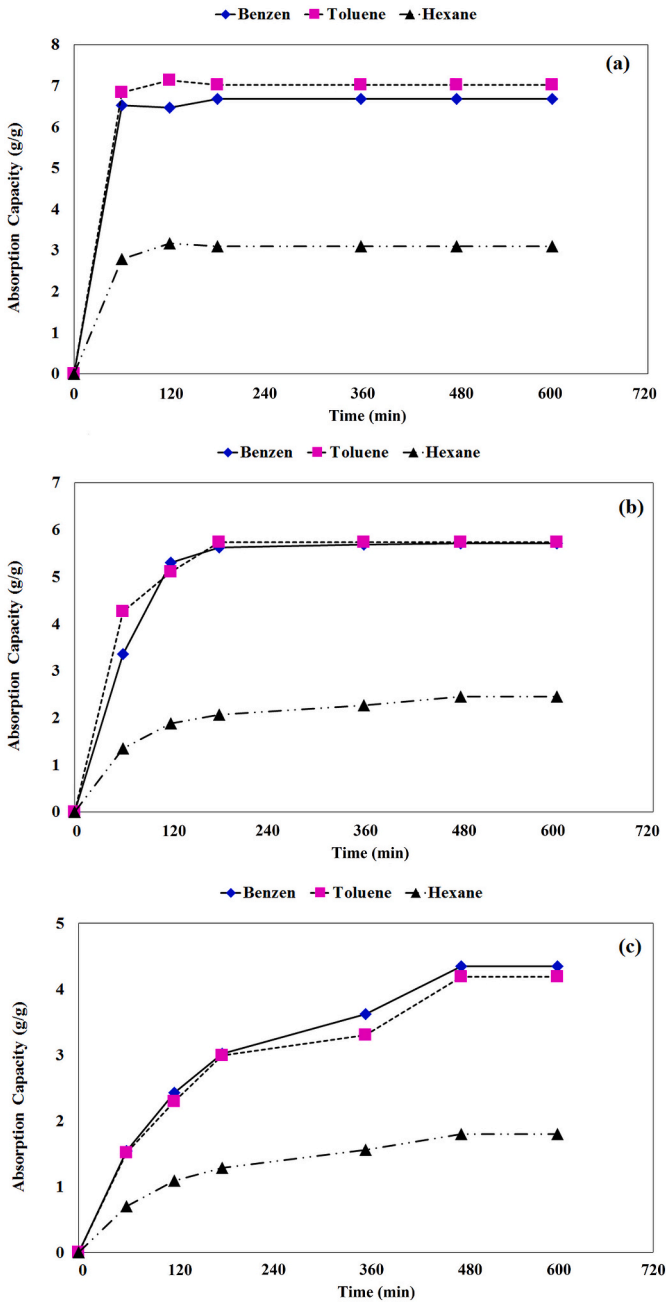

Fig. 6. Absorption kinetics of the polyHIPEs in different solvent mediums. (a) PMBS-1, (b) PMBS-2, and (c) PMBS-3.

pseudo-first order and pseudo second-order rate equations given in Eqs. (2) and (3), respectively [63].

$$ln\,(q_e - q_t) = lnq_e - k_1 t \quad (2)$$

$$t/q_t = 1/(k_2\, q_e^{\,2}) + t/q_e \quad (3)$$

where q_e (g/g) and q_t (g/g) are the absorption capacities at equilibrium and time t (min), respectively. k_1 is the pseudo-first order and k_2 is the pseudo-second order rate constants. While, pseudo-first order kinetic model was not to be fit with the experimental data, pseudo-second order model was found to be in a good correlation with the experimental data. The pseudo-second order kinetic plots of the solvent absorption of polyHIPEs are presented in Fig. 7, while the kinetic parameters are tabulated in Table 5. As can be seen from the given plots and the presented kinetic data in the table, R-square (R^2) values that are close to 1 is

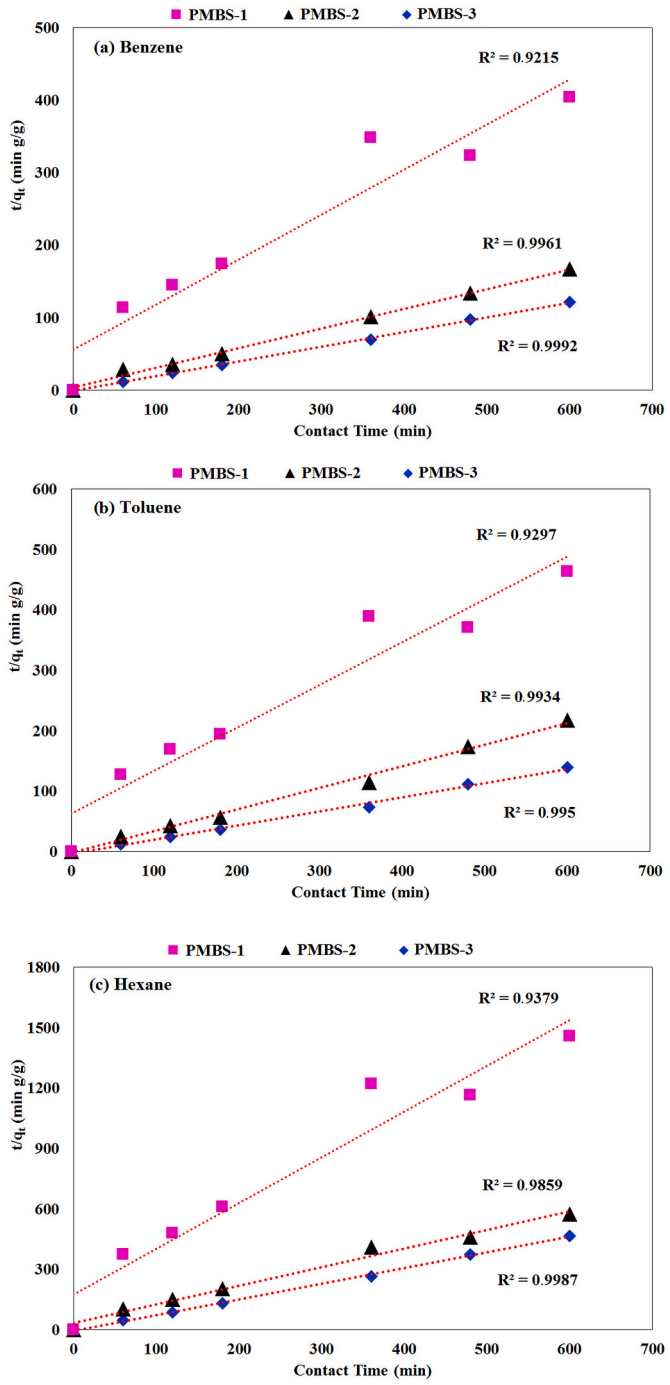

Fig. 7. The pseudo-second order of absorption kinetics of polyHIPEs: (a) Benzene, (b) toluene, and (c) hexane.

Table 5
Pseudo-second order kinetic parameters for the solvent absorption of polyHIPEs.

	Solvent	Rate Constant k_2 (g/g min)	R^2
PMBS-1	Benzene	0.0069	0.9215
	Toluene	0.0080	0.9297
	Hexane	0.0296	0.9379
PMBS-2	Benzene	0.0163	0.9961
	Toluene	0.0867	0.9934
	Hexane	0.0252	0.9859
PMBS-3	Benzene	0.0555	0.9992
	Toluene	0.0181	0.9950
	Hexane	0.1673	0.9987

showing the good agreement between the kinetic model and the experimental data. Considering the rate constants, it can be concluded that the order of absorption rate was quite different for the polyHIPEs. For PMBS-1 absorption rate was found to be change in the order of hexane > toluene > benzene. On the other hand, the order of absorption rate was respectively found to be toluene > hexane > benzene and hexane > benzene > toluene for PMBS-2 and PMBS-3. In addition to all, it was determined that the fastest absorption was carried out by PMBS-3 in hexane. In general, it is expected that the solvent which has the lowest polarity absorbed faster [61]. Since the relative solvent polarities was changing in the order of benzene > toluene > hexane, it is not surprising that hexane being absorbed faster within the polyHIPEs. However, the data obtained show that only PMBS-1 fits this order. In addition, it was found that PMBS-1 exhibited slower absorption as compared to PMBS-2 and PMBS-3. When the polarity of the solvent is low, absorption process is limited with the surface of the sorbent material and equilibrium is reached fast, which means absorption rate is high. On the other hand, when the polarity increased a two-stage mechanism is involved. In the first step absorbent molecules interact with the surface of the sorbent, then in the second step they diffused into the matrix. As expected, this mechanism is slower but results in higher amount of absorption [61].

4. Conclusions

In this study, we reported the first examples of terpene-based polyHIPE sorbents in the literature to demonstrate the applicability in spilled oil recovery. Sorbents were prepared by the copolymerization of *β*-myrcene and 1,3-butanediol dimethacrylate (BDDMA) in water-in-oil (w/o) type high internal phase emulsions (HIPEs). In this way, polyHIPE sorbents were obtained by using up to 95 vol% *β*-myrcene in the monomer composition. We showed that pore morphology of the resulting polyHIPEs was determined by the combination of several parameters including monomer composition and crosslinking degree. On the other hand, we also demonstrated that mechanical processes such as purification and drying have also remarkable influence on the formation of pores. Thanks to the contributions of isoprene and BDDMA units to chain flexibility, resulting polyHIPEs showed an elastic behavior. Due to the hydrophobic nature of the sorbents and low-crosslinking degree as in rubbers, the swelling capacity of the polyHIPEs was excellent against toluene, hexane, and benzene. Conclusively, we showed that emulsion templating can be used for the design of new sorbent materials by using sustainable bio-derived sources.

Supplementary data to this article can be found online at https://doi.org/10.1016/j.reactfunctpolym.2021.104912.

Authorship statement

All persons who meet authorship criteria were listed as authors, and all authors certified that they have participated sufficiently in the work to take public responsibility for the content, including participation in the concept, design, analysis, writing, or revision of the manuscript. Furthermore, each author certifies that this material or similar material has not been and will not be submitted to or published in any other publication before its appearance in the Reactive and Functional Polymers.

Declaration of Competing Interest

The authors declare that they have no known competing financial interests or personal relationships that could have appeared to influence the work reported in this paper.

References

[1] J.A. Fay, Model of spills and fires from LNG and oil tankers, J. Hazard. Mater. 96 (2003) 171–188, https://doi.org/10.1016/S0304-3894(02)00197-8.

[2] P. Dalling, I. Singsaas, M. Reed, O. Hansen, Experiences in dispersant treatment of experimental oil spills, Spill. Sci. Technol. Bull. 7 (2002) 201–213, https://doi.org/10.1016/S1353-2561(02)00061-0.

[3] S.P. Zhu, D. Strunin, Modelling the confinement of spilled oil with floating booms, Spill. Sci. Technol. Bull. 25 (2001) 713–729, https://doi.org/10.1016/S0307-904X(01)00008-7.

[4] C.A. Page, J.S. Bonner, T.J. McDonald, R.L. Autenrieth, Behaviour of a chemically dispersed oil in a wetland environment, Water Res. 36 (2002) 3821–3833, https://doi.org/10.1016/S0043-1354(02)00079-9.

[5] P.J. Strong, J.E. Burgess, Treatment methods for wine-related and distillery wastewaters review, Bioremediat. J. 12 (2008) 70–87, https://doi.org/10.1080/10889860802060063.

[6] M.H. Fulekar, M. Geetha, Bioremediation of chlorpyrifos by *Pseudomonas aeruginosa* using scale up technique, J. Appl. Biosci. 12 (2008) 657–660.

[7] D. Singh, M.H. Fulekar, Benzene bioremediation using cow dung microflora in two phase partitioning bioreactor, J. Hazard. Mater. 175 (2009) 336–343, https://doi.org/10.1016/j.jhazmat.2009.10.008.

[8] L. Wojnarovits, C.S.M. Földváry, E. Takács, Radiation-induced grafting of cellulose for adsorption of hazardous water pollutants: a review, Radiat. Phys. Chem. 79 (2010) 848–862, https://doi.org/10.1016/j.radphyschem.2010.02.006.

[9] G. Desmet, E. Takacs, L. Wojnarovits, J. Borsa, Cellulose functionalization via high-energy irradiation-initiated grafting of glycidyl methacrylate and cyclodextrin immobilization, Radiat. Phys. Chem. 80 (2011) 1358–1362, https://doi.org/10.1016/j.radphyschem.2011.07.009.

[10] K. Hemvichian, A. Chanthawong, P. Suwanmala, Synthesis and characterization of superabsorbent polymer prepared by radiation-induced graft copolymerization of acrylamide onto carboxymethyl cellulose for controlled release of agrochemicals, Radiat. Phys. Chem. 103 (2014) 167–171, https://doi.org/10.1016/j.radphyschem.2014.05.064.

[11] M. Zamparas, D. Tzivras, V. Dracopoulos, T. Ioannides, Application of sorbents for oil spill cleanup focusing on natural-based modified materials: a review, Molecules 25 (2020) 4522, https://doi.org/10.3390/molecules25194522.

[12] S. Askin, S. Kizil, H. Bulbul Sonmez, Hydrophobic cross-linked poly (dimethylsiloxane)-based sorbents for oil spill application, Macromol. Mater. Eng. 306 (2021) 2000556, https://doi.org/10.1002/mame.202000556.

[13] A. Erdem, Synthesis and characterization of polypropylene glycol-based novel organogels as effective materials for the recovery of organic solvents, J. Appl. Polym. Sci. 138 (2021) 49997, https://doi.org/10.1002/app.49997.

[14] M. Xue, R. Chitrakar, K. Sakane, T. Hirotsu, K. Ooi, Y. Yoshimura, Q. Feng, N. Sumida, Selective adsorption of thiophene and 1-benzothiophene on metal-ion-exchanged zeolites in organic medium, J. Colloid Interface Sci. 285 (2005) 487–492, https://doi.org/10.1016/j.jcis.2004.12.031.

[15] N. Sakdinun, P. Pattarapan, N. Chawalit, Comparative study on adsorptive removal of thiophenic sulfurs over Y and USY zeolites, Ind. Eng. Chem. Res. 47 (2008) 7405–7413, https://doi.org/10.1021/ie701785s.

[16] S.P. Hernandez, D. Fino, N. Russo, High performance sorbents for diesel oil desulfurization, Chem. Eng. Sci. 65 (2010) 603–609, https://doi.org/10.1016/j.ces.2009.06.050.

[17] S. Yang, L. Chen, L. Mu, B. Hao, P.C. Ma, Low cost carbon fiber aerogel derived from bamboo forthe adsorption of oils and organic solvents with excellent performances, RSC Adv. 5 (2015) 38470–38478, https://doi.org/10.1039/C5RA03701H.

[18] S.M. Sidik, A.A. Jalil, S. Triwahyono, S.H. Adam, M.A.H. Satar, B.H. Hameed, Modified oil palm leaves adsorbent with enhanced hydrophobicity for crude oil removal, Chem. Eng. J. 203 (2012) 9–18, https://doi.org/10.1016/j.cej.2012.06.132.

[19] J. Wang, Y. Zheng, A. Wang, Investigation of acetylated kapok fibers on the sorption of oil in water, J. Environ. Sci. 25 (2013) 246–253, https://doi.org/10.1016/S1001-0742(12)60031-X.

[20] C. Kantipuly, S. Katragadda, A. Chow, H.D. Gesser, Chelating polymers and related supports for separation and preconcentration of trace metals, Talanta 37 (1990) 491–517, https://doi.org/10.1016/0039-9140(90)80075-Q.

[21] T. Kaliyappan, P. Kannan, Coordination polymers, Prog. Polym. Sci. 25 (2000) 343–370, https://doi.org/10.1016/S0079-6700(00)00005-8.

[22] N. Arsalani, R. Rakh, E. Ghasemi, A.A. Entezami, Removal of Ni(II) from synthetic solutions using new amine-containing resins based on polyacrylonitrile, Iran. Polym. J. 18 (2009) 623–632.

[23] Y. Xie, C.A.S. Hill, Z. Xiao, H. Militz, C. Mai, Silane coupling agents used for natural fiber/polymer composites: a review, Compos. Part A Appl. Sci. Manuf. 41 (2010) 806–819, https://doi.org/10.1016/j.compositesa.2010.03.005.

[24] A.A. Al-Majed, A.R. Adebayo, M.E. Hossain, A sustainable approach to controlling oil spills, J. Environ. Manag. 113 (2012) 213–227, https://doi.org/10.1016/j.jenvman.2012.07.034.

[25] T. Zhang, R.A. Sanguramath, S. Israel, M.S. Silverstein, Emulsion templating: porous polymers and beyond, Macromolecules 52 (2019) 5445–5479, https://doi.org/10.1021/acs.macromol.8b02576.

[26] A.Y. Sergienko, H.W. Tai, M. Narkis, M.S. Silverstein, Polymerized high internal-phase emulsions: properties and interaction with water, J. Appl. Polym. Sci. 84 (2002) 2018–2027, https://doi.org/10.1002/app.10555.

[27] T. Zhang, M.S. Silverstein, Highly porous, emulsion templated, zwitterionic hydrogels: amplified and accelerated uptakes with enhanced environmental sensitivity, Polym. Chem. 9 (2018) 3479–3487, https://doi.org/10.1039/C8PY00588E.

[28] E. Yüce, E.H. Mert, S. Şen, S. Saygı, N. San, Properties and applications of nanoclay reinforced open porous polymer composites, J. Appl. Polym. Sci. 134 (2017) 45522, https://doi.org/10.1002/app.45522.

[29] A. Szczurek, V. Fierro, M. Thebault, A. Pizzi, A. Celzard, Structure and properties of poly(furfuryl alcohol)-tannin polyHIPEs, Eur. Polym. J. 78 (2016) 195–212, https://doi.org/10.1016/j.eurpolymj.2016.03.037.

[30] A. Szczurek, A. Martinez de Yuso, V. Fierro, A. Pizzi, A. Celzard, Tannin-based monoliths from emulsion-templating, Mater. Eng. 79 (2015) 115–126, https://doi.org/10.1016/j.matdes.2015.04.020.

[31] Foulet, M. Birot, R. Backov, G. Sonnemann, H. Deleuze, Preparation of hierarchical porous carbonaceous foams from Kraft black liquor, Mater. Today Commun. 7 (2016) 108–116, https://doi.org/10.1016/j.mtcomm.2016.04.005.

[32] J.J. Blaker, K.Y. Lee, X.X. Li, A. Menner, A. Bismarck, Renewable nanocomposite polymer foams synthesized from Pickering emulsion templates, Green Chem. 11 (2009) 1321–1326, https://doi.org/10.1039/B913740H.

[33] J. Meehan-Atrash, W. Luo, R.M. Strongin, Toxicant formation in dabbing: the terpene story, ACS Omega 2 (2017) 6112–6117, https://doi.org/10.1021/acsomega.7b01130.

[34] H. Ho, W.H. Griest, M.R. Guerin, Application of the blind assay to biological activity and tobacco smoke terpenes, Anal. Chem. 48 (1976) 2223–2226, https://doi.org/10.1021/ac50008a044.

[35] A. Stamm, M. Tengdelius, B. Schmidt, J. Engström, P.O. Syrén, L. Fogelström, E. Malmström, Chemo-enzymatic pathways toward pinene-based renewable materials, Green Chem. 21 (2019) 2720–2731, https://doi.org/10.1039/C9GC00718K.

[36] R.H. Kollarigowda, S. Abraham, One-Pot synthesis: polymers, hydrogel and nanoparticles from natural extracted green materials, ChemRxivTM (2019), https://doi.org/10.26434/chemrxiv.7638074.v1.

[37] B. Hird, J.C. Dyer, D.H. Melik, Biodegradable articles made from certain trans-polymers and blends thereof with other biodegradable components, United States Patent (1998) US005759569A.

[38] J.L. Cawse, J.L. Stanford, R.H. Still, Polymers from renewable sources: 5. Myrcene-based polyols as rubber-toughening agents in glassy polyurethanes, J. Appl. Polym. Sci. 28 (1987) 368–374, https://doi.org/10.1016/0032-3861(87)90187-X.

[39] Z. Hazan, S. Amselem, Compositions of Polymeric Myrcene, United States Patent (2014) US008722105B2.

[40] E.H. Mert, B. Kekevi, Synthesis of polyHIPEs through high internal phase emulsions of β-myrcene, Colloid Polym. Sci. 298 (2020) 1423–1432, https://doi.org/10.1007/s00396-020-04730-4.

[41] E.H. Mert, B. Kekevi, Synthesis of β-myrcene based macroporous nanocomposite foams: altering the morphological and mechanical properties by using organo-modified nanoclay, J. Appl. Polym. Sci. 138 (2021) 50074, https://doi.org/10.1002/app.50074.

[42] V. Vašková, M. Stillhammerová, J. Bartoň, Inverse microemulsion polymerization of acrylamide in the presence of bi-unsaturated vinyl monomers, Chem. Pap. 48 (1994) 355–361.

[43] H. Tobita, A.E. Hamielec, Control of network structure in free-radical crosslinking copolymerization, Polymer 33 (1992) 3647–3657, https://doi.org/10.1016/0032-3861(92)90651-C.

[44] L. Trumbo, Free radical copolymerization behavior of myrcene I. copolymers with styrene, methyl methacrylate or p-fluorostyrene, Polym. Bull. 31 (1993) 629–636, https://doi.org/10.1007/BF00300120.

[45] J. Hilschmann, G. Kali, Bio-based polymyrcene with highly ordered structure via solvent free controlled radical polymerization, Eur. Polym. J. 73 (2015) 363–373, https://doi.org/10.1016/j.eurpolymj.2015.10.021.

[46] W. Busby, N.R. Cameron, C.A.B. Jahoda, Tissue engineering matrixes by emulsion templating, Polym. Int. 51 (2002) 871–881, https://doi.org/10.1002/pi.934.

[47] O. Kulygin, M.S. Silverstein, Porous poly(2-hydroxyethyl methacrylate) hydrogels synthesized within high internal phase emulsions, Soft Matter 3 (2007) 1525–1529, https://doi.org/10.1039/b711610a.

[48] J. Majer, E. Žagar, P. Krajnc, S. Kovačič, In situ hyper-cross-linking of glycidyl methacrylate–based polyHIPEs through the amine-enriched high internal phase emulsions, Colloid Polym. Sci. 297 (2019) 239–247, https://doi.org/10.1007/s00396-018-4455-z.

[49] A. Menner, A. Bismarck, New evidence for the mechanism of the pore formation in polymerising high internal phase emulsions or why polyHIPES have an interconnected pore network structure, Macromol. Symp. 242 (2006) 19–24, https://doi.org/10.1002/masy.200651004.

[50] P. Sarkar, A.K. Bhowmick, Green approach toward sustainable polymer: Synthesis and characterization of poly(myrcene-co-dibutyl itaconate), ACS Sustain. Chem. Eng. 4 (2016) 2129–2141, https://doi.org/10.1021/acssuschemeng.5b01591.

[51] E. Grune, J. Bareuther, J. Blankenburg, M. Appold, L. Shaw, A.H.E. Müller, G. Floudas, L.R. Hutchings, M. Gallei, H. Frey, Towards bio-based tapered block copolymers: the behaviour of myrcene in the statistical anionic copolymerisation, Polym. Chem. 10 (2019) 1213–1220, https://doi.org/10.1039/C8PY01711E.

[52] N.R. Cameron, High internal phase emulsion templating as a route to well-defined porous polymers, Polymer 46 (2005) 1439–1449, https://doi.org/10.1016/j.polymer.2004.11.097.

[53] H.H. Mert, M.S. Mert, E.H. Mert, A statistical approach for tailoring the morphological and mechanical properties of polystyrene polyHIPEs: looking through experimental design, Mater. Res. Express 6 (2019) 115306, https://doi.org/10.1088/2053-1591/ab437f.

[54] E.H. Mert, H.H. Mert, Preparation of polyHIPE nanocomposites: revealing the influence of experimental parameters with the help of experimental design approach, Polym. Compos. 42 (2020) 724–738, https://doi.org/10.1002/pc.25861.

[55] P. Sarkar, A.K. Bhowmick, Synthesis, characterization and properties of a biobased elastomer: polymyrcene, RSC Adv. 4 (2014) 61343–61354, https://doi.org/10.1039/c4ra09475a.

[56] P. Sarkar, A.K. Bhowmick, Terpene based sustainable elastomer for low rolling resistance and improved wet-grip application: synthesis, characterization and properties of poly(styrene-co-myrcene), ACS Sustain. Chem. Eng. 4 (2016) 5462–5474, https://doi.org/10.1021/acssuschemeng.6b01038.
[57] P. Sahu, A.K. Bhowmick, G. Kali, Terpene based elastomers: synthesis, properties, and applications, Processes 8 (2020) 553, https://doi.org/10.3390/pr8050553.
[58] A. Phenix, The swelling or artists' paint in organic solvents. Part 2, Comparative swelling powers of selected organic solvents and solvent mixtures, J. Am. Inst. Conserv. 41 (2002) 61–90, https://doi.org/10.1179/019713602806082647.
[59] T. Ono, T. Sugimoto, S. Shinkai, K. Sada, Lipophilic polyelectrolyte gels as super-absorbent polymers for nonpolar organic solvents, Nat. Mater. 6 (2007) 429–433, https://doi.org/10.1038/nmat1904.
[60] N. Yacob, K. Hashim, Morphological effect on swelling behavior of hydrogel, AIP Conf. Proc. 153 (2014) 1584, https://doi.org/10.1063/1.4866123.
[61] M.R. Krishan, Y.F. Aldawsari, E.H. Alsharaeh, Three-dimensionally cross-linked styrene-methyl methacrylate-divinyl benzene terpolymer networks for organic solvents and crude oil absorption, J. Appl. Polym. Sci. 138 (2020) 49942, https://doi.org/10.1002/app.49942.
[62] P.J. Flory, Principles of Polymer Chemistry; Baker Lectures 1948, Cornell University Press, Ithaca, New York, 1953.
[63] H. Moussout, H. Ahlafi, M. Aazza, H. Maghat, Critical of linear and nonlinear equations of pseudo-first order and pseudo-second order kinetic models, Karbala Int. J. Mod. Sci. 4 (2018) 244–254, https://doi.org/10.1016/j.kijoms.2018.04.001.